Differentiation of chemically induced liver progenitor cells to cholangiocytes: Investigation of the optimal conditions

Yu Huang,[1,2] Yusuke Sakai,[1,3] Takanobu Hara,[1] Takeshi Katsuda,[4] Takahiro Ochiya,[4] Wei-Li Gu,[2] Daisuke Miyamoto,[1,3] Takashi Hamada,[1] Kengo Kanetaka,[1] Tomohiko Adachi,[1] and Susumu Eguchi[1,*]

Department of Surgery, Nagasaki University Graduate School of Biomedical Sciences, 1-7-1 Sakamoto, Nagasaki 852-8501, Japan,[1] Department of Surgery, Guangzhou First People's Hospital, School of Medicine, South China University of Technology, Guangzhou 510180, China,[2] Department of Chemical Engineering, Faculty of Engineering, Graduate School, Kyushu University, 744 Motooka, Nishi-ku, Fukuoka 819-0395, Japan,[3] and Division of Molecular and Cellular Medicine, National Cancer Center Research Institute, 5-1-1 Tsukiji, Chuo-ku, Tokyo 104-0045, Japan[4]

Chemically induced liver progenitor (CLiP) cells, converted *in vitro* from mature hepatocytes, possess the bipotentiality to differentiate into both hepatocytes and cholangiocytes. Here, we aimed to investigate the optimal conditions for bile duct (BD) induction from rat CLiPs. A two-step induction protocol was used for the differentiation of cholangiocytes. We investigated the effects of passage number, preincubation times, Matrigel, and mouse embryonic fibroblast (MEF) feeder cells on the induction of cholangiocytes. Earlier passages of CLiPs were better for BD induction compared with stable CLiPs. Extending the preincubation time of CLiPs before induction delayed the formation of the BD. Matrigel provided cells with space to form three-dimensional (3D) structures, but the long-term use of Matrigel from the induction step did not benefit the differentiation of CLiPs to cholangiocytes. MEF feeder cells, through the Jag/Notch pathway, affected BD formation and function, as well as gene and protein expression. CLiPs were a good cell source for cholangiocyte differentiation under appropriate conditions and may offer a key vehicle for the study of cholangiopathies *in vitro*.

© 2020, The Society for Biotechnology, Japan. All rights reserved.

[Key Words: Chemically induced liver progenitor cells; Cholangiocytes; Culture conditions; Bile duct structures; Liver progenitor cells]

Cholangiocytes, the epithelial cells that line intrahepatic and extrahepatic bile ducts (BDs), are highly specialized cells residing in a complex anatomic niche where they participate in bile production and homeostasis (1,2). Cholangiocytes are damaged in a variety of human diseases termed cholangiopathies, often causing advanced liver failure. To gain a better understanding of cholangiopathies, the development of methods to study cholangiocytes is required. However, this has proved to be difficult due to the lack of access to cholangiocytes and relatively low percentage of these cells in the liver (3). Hence, many researchers have attempted to generate cholangiocytes from induced pluripotent stem cells (iPSCs) or liver progenitor cells (LPCs) for use in regenerative medicine (4—7).

In 2017, the Ochiya group in Japan published their significant findings regarding chemically induced liver progenitor cells (CLiPs) (8). CLiPs are converted *in vitro* from mature hepatocytes with a chemical cocktail named YAC. Similar to LPCs, CLiPs possess the bipotentiality to differentiate into both hepatocytes (8,9) and cholangiocytes (8) and form three-dimensional (3D) structures (10) under special culture conditions. Therefore, CLiPs can be used to study hepatocytes and cholangiocytes (11). In their work, they established a two-step protocol to generate ductular structures.

Good and stable induction conditions will facilitate the application of BDs differentiated from CLiPs. Here, we investigate the optimal conditions for BD induction using rat CLiPs. Four factors (passage number of CLiPs, length of preincubation before starting the induction process, use of Matrigel, and use of mouse embryonic fibroblasts (MEF) feeder cells) affected the efficiency of BD induction. Our optimal conditions for BD induction using rat CLiPs provide a platform for future studies of cholangiopathies and other applications of cholangiocytes.

MATERIALS AND METHODS

Isolation of primary rat hepatocytes　Primary mature hepatocytes were isolated from 7-week-old male Wistar rats (Charles River Laboratories Japan, Yokohama, Japan) using a modified two-step perfusion method as previously described (12,13). Briefly, after perfusion with a Ca^{2+}-free Hank's/EGTA solution through the portal vein, the liver was perfused with ∼130 mL of Hanks solution containing 130 units/mL collagenase at 20—30 mL/min. The liver was extracted and mechanically minced with a surgical knife. The minced liver was then filtered twice by a four-layer cotton mesh and 45 μm stainless steel mesh. Then, the suspension was purified thrice in DMEM high-glucose medium by centrifugation at 50 $\times g$ for 2 min at 4°C. The cells were then resuspended in 40% Percoll solution (GE Healthcare, Tokyo, Japan), and the dead cells were removed via centrifugation at 50 $\times g$ for 20 min. We performed all experiments using purified hepatocytes that were at least 90% viable, which was determined using trypan blue. Animal studies were performed in compliance with the guidelines of the Animal Ethics Committee at Nagasaki University.

* Corresponding author. Tel.: +81 95 819 7316; fax: +81 95 819 7319.
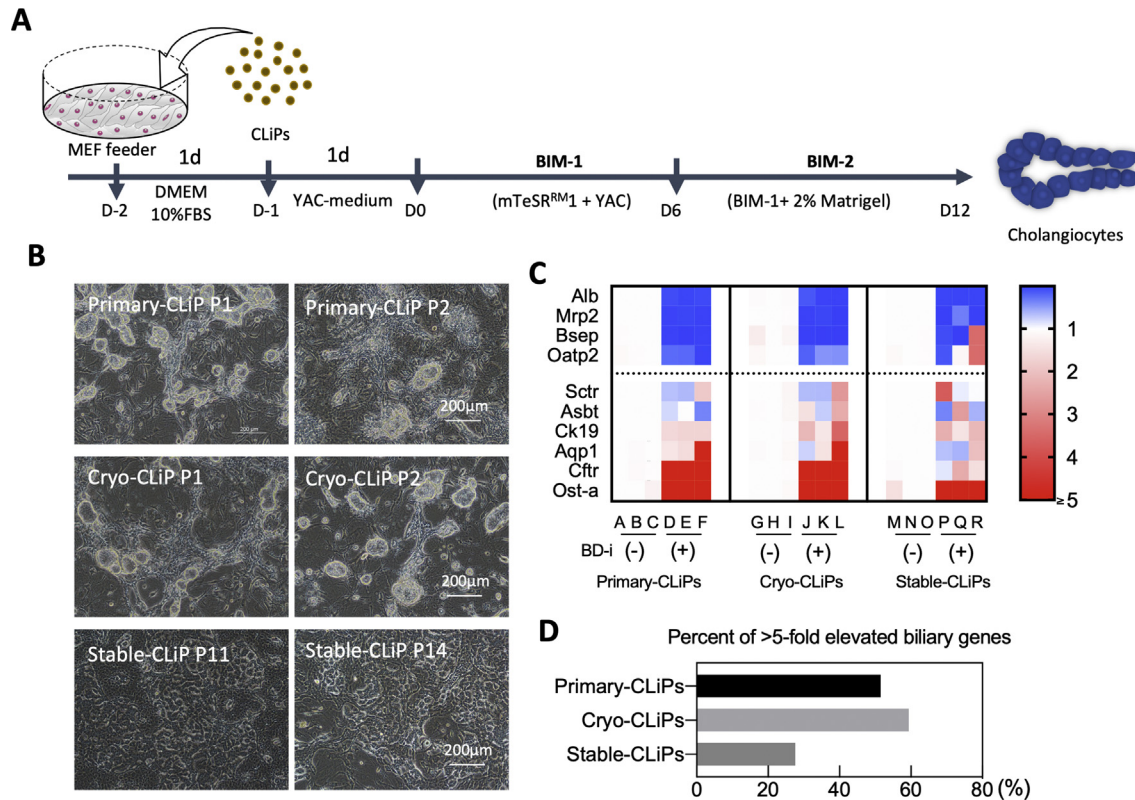E-mail address: sueguchi@nagasaki-u.ac.jp (S. Eguchi).

FIG. 1. The passaging of CLiPs affects bile duct (BD) formation. (A) The schematic of the BD induction protocol. (B) Representative cell morphologies of BDs at day 12 from primary-CLiPs (P1 and P2), cryopreserved CLiPs (cryo-CLiPs, P1, and P2), and stable-CLiPs, which were passaged more than 10 times. (C) The heat map of the gene profile in primary-CLiPs, cryo-CLiPs, and stable-CLiPs used for BD induction (BD-i (+)). The samples from the same CLiPs cultured in YAC-medium were set as the control group (BD-i (−)). The expression levels were determined by qRT-PCR, calculated using the 2(−ΔΔCt) method, and compared to the housekeeping gene *Actb*. The color bar represents the levels compared to the control group, which was set as 1. (D) The percentages of the >5-fold elevated biliary genes among the >1.5-fold upregulated genes in primary-CLiPs, cryo-CLiPs, and stable-CLiPs.

Conversion of hepatocytes into CLiPs   The differentiation protocol has been previously described (8,11). Briefly, approximately 6×10^5 freshly isolated hepatocytes were seeded on 100 mm collagen-coated dishes (Asahi Techno Glass, Tokyo, Japan) in differentiation medium consisting of DMEM/F12 containing 2.4 g/L NaHCO$_3$ and L-glutamine supplemented with 10 μM Y-27632, 0.5 μM A-83-01, 3 μM CHIR99021, 5 mM HEPES, 30 μg/mL L-proline, 0.5 mg/mL BSA, 10 ng/mL epidermal growth factor, insulin-transferrin-serine-X, 0.1 μM dexamethasone (Dex), 10 mM nicotinamide, 1 mM ascorbic acid-2 phosphate, 100 U/mL penicillin, and 100 mg/mL streptomycin. The medium was changed 1 day after seeding and every other day thereafter. The cells reached 90% confluency within 2 weeks. In order to emphasize the key role of the three small chemicals Y-27632, A-83-01, and CHIR99021, we termed this differentiation medium YAC-medium.

Subculture of CLiPs   The cells were passaged once they reached 90% confluency. After washing with phosphate buffered saline (PBS), cells were dissociated with 2 mL of TrypLE Express (Gibco, Thermo Fisher Scientific, Waltham, MA, USA) for 15 min at 37°C. The equivalent volume of pre-culture medium was added, and the cells were transferred to a 15 mL conical tube and centrifuged at 220 ×g for 5 min. The cell pellet was resuspended in 5 mL of culture medium, and the total number of cells and percent viability were determined using a hemocytometer. For the next subculture, 2×10^6 cells were seed on 100 mm collagen-collated dishes in YAC-medium containing 5% FBS. For cryopreserved cells, about $2-5 \times 10^6$ cells were frozen in TC-Protector medium (KAC, Kyoto, Japan) at −80°C for 3–7 days and then transferred to liquid nitrogen for long-term storage. We termed the first passage of CLiPs as P1, the second passage cells as P2, and cells that were passaged >10 times were referred to as stable CLiPs. P1 CLiPs were cryopreserved. Recovered P1 cells were termed as cryo-CLiPs P1, and the subcultured cells were termed cryo-CLiPs P2. Cells were cultured in the YAC-medium presented above.

Differentiation of CLiPs into biliary cells   We used the two-step induction protocol for biliary cell differentiation as previously described (8). One day before obtaining the CLiP suspension, we used commercial MEFs (cat. no. PMEF-N, Merck Millipore, Tokyo, Japan) to generate MEF feeder layers on collagen-coated 12-well plates in DMEM with 10% FBS. We set 5×10^4 cells as the Low-MEF condition and 2×10^5 cells as the High-MEF condition. The next day, we seeded CLiPs onto the MEF feeder cells at a density of 5×10^5 cells/well in YAC-medium supplemented with 5% FBS, and the cells were cultured for 1–10 days. We then replaced the medium every 2 days with biliary epithelial cell induction medium (BIM) for 6 days, followed by BIM supplemented with 2% growth factor-reduced Matrigel (lot: 354230, Corning, Tokyo, Japan) for another 6–10 days to facilitate the maturation of cholangiocytes and formation of BDs. The BIM consisted of mTeSR1 medium (no. 85850, STEMCELL Technologies, Vancouver, Canada) supplemented with 10 μM of Y-27632, 0.5 μM of A-83-01, and 3 μM of CHIR99021.

Quantitative real-time PCR   Total RNA was extracted using an RNA isolation kit (NucleoSpin RNA II; Macherey-Nagel, Düren, Germany), as previously reported (10). cDNAs were converted using a high-capacity cDNA reverse transcription kit (Applied Biosystems, Tokyo, Japan). Then, PCRs were performed using a TaqMan Fast Universal PCR Master Mix (Applied Biosystems) and an Applied Biosystems StepOnePlus Real-Time PCR System according to the manufacturer's instructions. The thermocycling conditions were 95°C for 20 s, followed by 40 cycles of 95°C for 1 s and 60°C for 20 s. Cycle threshold (Ct) values were automatically determined by the StepOnePlus Real-Time PCR System. Actin-beta (*Actb*) was used as the housekeeping gene and internal control. Data were analyzed using the 2-(−ΔΔCt) method. The TaqMan primers used for quantitative real-time PCR (qRT-PCR) are listed in Table S1.

In order to test whether the rat TaqMan cross-react with mouse sample or not, we checked the mouse embryonic fibroblast (MEF) cell samples with rat TaqMan which used in this study and compared with the mouse *Actb* (Actb_m) TaqMan. Followed by 40 cycles of running, the cycle threshold (Ct) values were automatically determined by the StepOnePlus Real-Time PCR System. As shown in Fig. S1A, the mean Ct value of Actb_m was 21, two of the markers (*Sox9* and *Ck7*) ranges at 30 to 35 in Ct value, five markers (*Ck19*, *Ggt1*, *Gpbar*, *Mdr1*, and *Alb*) ranged 35 to 40 in Ct value. The other 12 markers were undetermined. As we know that the higher Ct value is, the lower expression of this gene. We also calculated the relative expression level via 2-(−ΔCt) method compared with Actb_m which was set as 1. The data showed that the cross-reacted markers presented extremely lower level (almost zero) compared to Actb_m (Fig. S1B). Therefore, most rat TaqMan did not cross react with MEF samples or with few crosslinking to MEF samples.

Immunofluorescence staining   Cells were fixed with 4% paraformaldehyde at room temperature (RT) for 10 min, permeabilized with 0.1% Triton X-100 (Sigma–Aldrich, Tokyo, Japan) in PBS for 10 min, and blocked in PBS containing 1% BSA for 1 h at RT. Cells were incubated with primary antibodies at 4°C overnight. After washing the cells twice with PBS, cells were incubated with the appropriate
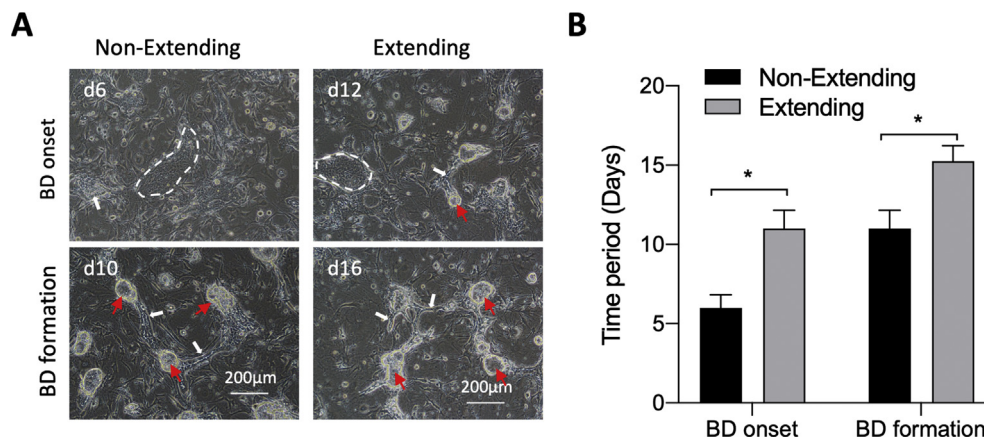
A

B

FIG. 2. Extending the preincubation time of CLiPs delays the formation of the bile duct (BD). (A) Representative cell morphologies at the time of BD onset and formation in non-extending and extending cases. BD onset was defined as the period from the beginning to the emergence of the BD, whereas BD formation was defined as the period required for the formation of tubular and cystic structures in all of the cells. The white and red arrows represent the tubular BDs and cystic BDs, respectively. The dotted line represents the area of undifferentiated CLiPs. (B) The comparison of the time periods of BD onset and formation in non-extending and extending cases (lot = 4, n = 4). Data are shown as the mean ± s.d. and were analyzed with a two-tailed Mann−Whitney U test, $^*p < 0.05$.

secondary antibodies for 2 h at RT. The antibodies, which we diluted in PBS + 1% BSA, are listed in Table S2. Nuclei were stained with 4',6-diamidino-2-phenylindole (Dojindo Laboratories, Kumamoto, Japan) for 30 min. Images were captured using a confocal laser scanning microscope (Olympus Corporation, Tokyo, Japan).

Rhodamine 123 dye assay   After washing once with HBSS, live cells were incubated with HBSS containing 100 μM of rhodamine 123 (both from Sigma−Aldrich, Japan) for 30 min at 37°C and then washed twice with HBSS. The stained cells were then visualized using a confocal microscope (Olympus Corporation).

Measurements of fluorescence intensity   The fluorescence intensities of the dyes along the indicated lines and the graphs of fluorescent values were measured and generated using ImageJ software (https://imagej.nih.gov/ij/index.html) as previously described.

Statistical analysis   All data are expressed as the mean ± standard deviations (s.d.). Statistical analyses were performed with GraphPad Prism 8.0 (GraphPad Software, Inc., San Diego, CA, USA) using the indicated tests presented in each figure legend. Differences with *p* values < 0.05 were considered statistically significant. The *n*-value refers to biologically independent replicates.

RESULTS

The passage number of CLiPs affects bile duct induction   We first analyzed the effect of passage number on cholangiocyte induction using a two-step induction method (Fig. 1A). We observed among the primary differentiated CLiP (primary-CLiPs), the cryopreserved primary-CLiP (cryo-CLiPs), and the CLiPs passaged more than 10 times, which we termed as stable-CLiPs. We analyzed hepatic and LPC genes among CLiP-P1, CLiP-P2 and stable-CLiP, compared to mature hepatocyte (MHs) samples. The data showed the decreased levels of *Alb* and *Hnf4α* in CLiP (Fig. S2A), and elevated the levels of *Sox9*, *Epcam*, *Afp* and *Krt19* in CLiPs compared to the MHs (Fig. S2B). The levels of those genes are comparable and showed no significant difference among CLiP-P1, CLiP-2 and stable-CLiP (Figs. S2A and B). Different cell morphologies were observed among them after induction. The earlier passages of CLiPs, including primary- and cryo-CLiPs, both formed typical tubular BD and cystic BD, while only monolayer structures were formed in the stable-CLiP cultures (Fig. 1B). We then compared the gene expression profiles among these CLiPs (Fig. 1C) compared with samples from the same CLiPs cultured in YAC-medium, which were used as the control group. Most of the biliary marker genes that were analyzed were upregulated after induction, whereas some biliary and almost all hepatic genes were downregulated. The number of biliary marker genes that increased by >1.5-fold was much higher in primary-

and cryo-CLiPs, with an average of 61.1% and 59.3%, respectively, than in stable-CLiPs with an average of 53.7%. Furthermore, the number of genes that were upregulated by >5-fold was higher in the earlier passages of CLiPs, including primary- and cryo-CLiPs, compared with stable-CLiPs (Fig. 1D). Besides, CLiP showed increase trends of *Ki67*, *Pcna* and *Ki67* genes, and showed significance in stable-CLiP (Fig. S2C). This quick proliferation rate in stable-CLiP may result in difficult in BD induction. Therefore, it is better to use the earlier passages of CLiPs for BD induction. Among the early passages, we recommend the use of primary-CLiPs to reduce the failure possibilities associated with cryo-CLiPs (Fig. S3). Primary-CLiPs P1 were used in all subsequent experiments unless indicated otherwise.

Extending the preincubation time of CLiPs before induction delays the formation of the bile duct   CLiPs were usually cultured in the differentiation medium for 1 day before starting the BD induction to allow the CLiPs to adhere to the dishes (Fig. 1A). In some cases, we found that the preincubation time was not sufficient for the CLiPs to attach to the dish, so we extended the preincubation time to increase the number of cells. To determine the optimal preincubation time, we compared the time required for BD onset (emerging of the BD) and typical BD formation (formation of tubular and cystic structures) (Fig. 2A). When the preincubation time was 1 day, BD onset and typical BD formation began on the 6th day and 10th day (on average), respectively (Fig. 2B). When the preincubation period was extended, BD onset and typical BD formation started on the 11th day and 15th day (on average), respectively (Fig. 2B). These data showed that extending the preincubation of CLiPs delayed the onset and formation of BD. Therefore, a 1-day preincubation period was used in all subsequent experiments unless indicated otherwise.

Matrigel affects bile duct formation   According to the previous two-step induction protocol, 2% Matrigel was applied as the second step for the last 6 days of culture (Matrigel 6 d). In order to determine the effect of Matrigel on BD formation, we compared the differences among the no-Matrigel, Matrigel 6 d, and Matrigel 12 d courses (Fig. 3A). Data showed that neither typical tubular nor cystic BD morphologies formed in the no-Matrigel course, while no typical tubular BD structures formed in the Matrigel 12 d course. In the Matrigel 6 d course, both typical tubular and cystic BD morphologies were formed (Fig. 3B). We also compared the levels of biliary gene expression among these courses (Fig. 3C). Hepatocyte nuclear factor 6 (*Hnf6*, also known
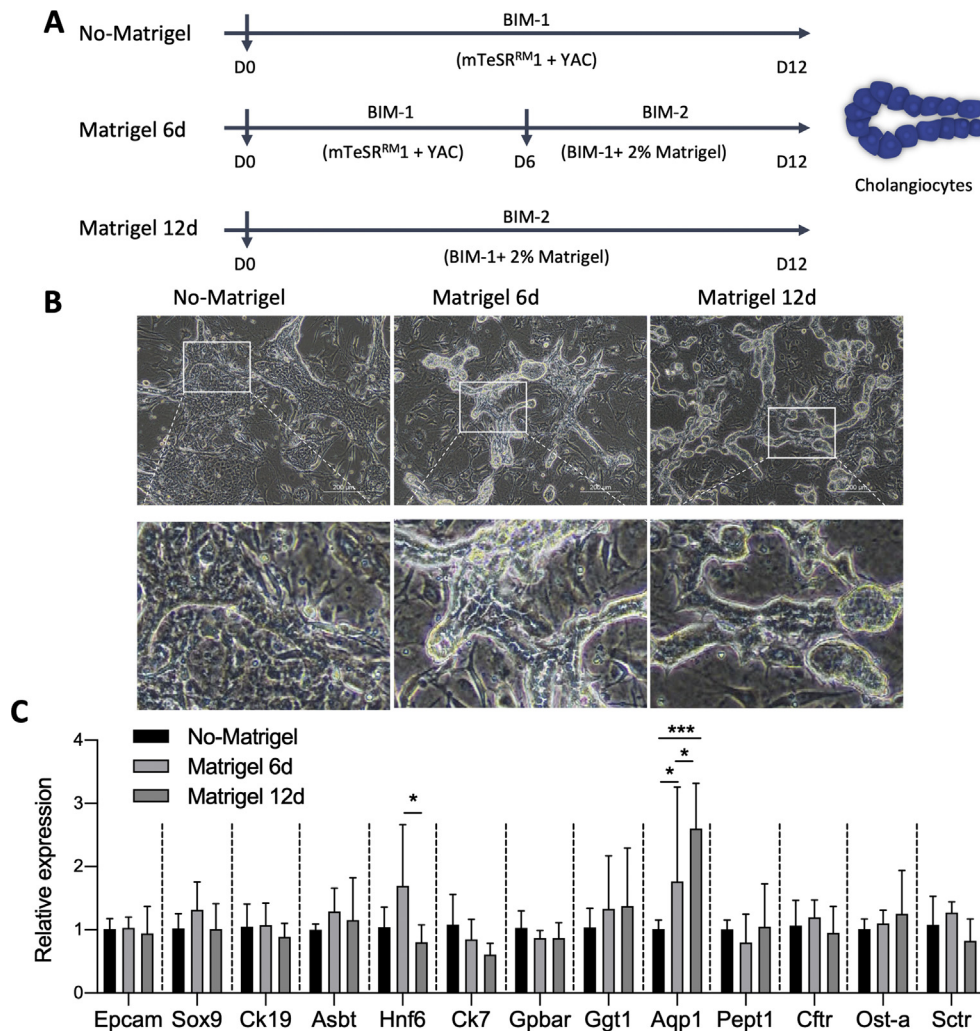
FIG. 3. Matrigel affects bile duct formation. (A) Schematic of the treatment with No-Matrigel, Matrigel 6 d, and Matrigel 12 d. (B) Representative cell morphologies at day 12 in no-Matrigel, Matrigel 6 d, and Matrigel 12 d courses. (C) The relative gene expression level of biliary markers in no-Matrigel, Matrigel 6 d, and Matrigel 12 d courses. Data were presented as the mean ± s.d. (lot = 2, n =5), and fold changes relative to the no-Matrigel course were normalized to the housekeeping gene *Actb*. Data were analyzed with a one-way ANOVA test, $^*p < 0.05$, $^{***}p < 0.001$.

as Onecut1) showed a relatively high level in the Matrigel 6 d course, while Aquaporin 1 (*Apq1*) showed a relatively high level in Matrigel 12 d course (Fig. 3C). Most of the biliary genes showed no differences among the three courses; however, the expression of SRY-Box Transcription Factor 9 (*Sox9*), Cytokeratin 19 (*Ck19*), *Ck7*, Cystic fibrosis transmembrane conductance regulator (*Cftr*), and Secretin receptor (*Sctr*) showed decreased trends in the Matrigel 12 d course. These data suggest that the addition of Matrigel provides cells with space to form 3D structures, but the long-term addition beginning from the induction step does not benefit the differentiation of CLiPs to cholangiocytes. For the next experiment, we used the Matrigel 6 d course as the standard protocol unless indicated otherwise.

MEF feeder cells affect BD formation and function, as well as gene and protein expression Previously, the CLiPs were cultured on MEF feeder layers. We then asked if the BD structures could form in the absence of MEFs. To this end, we seeded the CLiPs without MEFs (No-MEF) and in the presence of a low (Low-MEF) or high (High-MEF) number of MEFs. The cells were then cultured with induction medium for 12 days and compared with the CLiPs without MEFs cultured in YAC-medium for the same period as the control (Ctrl). There was no BD formation in the

Ctrl groups, and less typical BD structures formed in the No-MEF condition (Fig. 4A). Both typical tubular and cystic BD formation were analyzed in the Low- and High-MEF conditions (Fig. 4A). The number and the size (Fig. 4B) of cystic BDs gradually increased as the density of MEF feeder cells increased. In addition, the onset of BD formation in the High-MEF condition started earlier than that in the Low-MEF condition (Fig. S4). We also analyzed the expression of biliary marker genes with and without MEFs (Fig. 4C) and found that the levels were higher in the cells plated on MEF feeder layers compared with the No-MEF group. Similarly, the cells on the MEF feeder layers expressed an increased amount of biliary proteins compared with the No-MEF group (Fig. 5). Furthermore, we compared the transportation of rhodamine 123 dye among the different MEF feeder groups (Fig. 6A), which showed that BD structures formed in the High-MEF feeder group could transport a larger amount of dye (Fig. 6B).

MEFs affect BD formation through the Jag/Notch pathway Previous studies have shown that the Jag/Notch signaling pathway plays a key role in cholangiocyte genesis (14–18). Here, we asked if the MEF feeder cells promote BD formation by regulating Jag/Notch signaling in our system. The
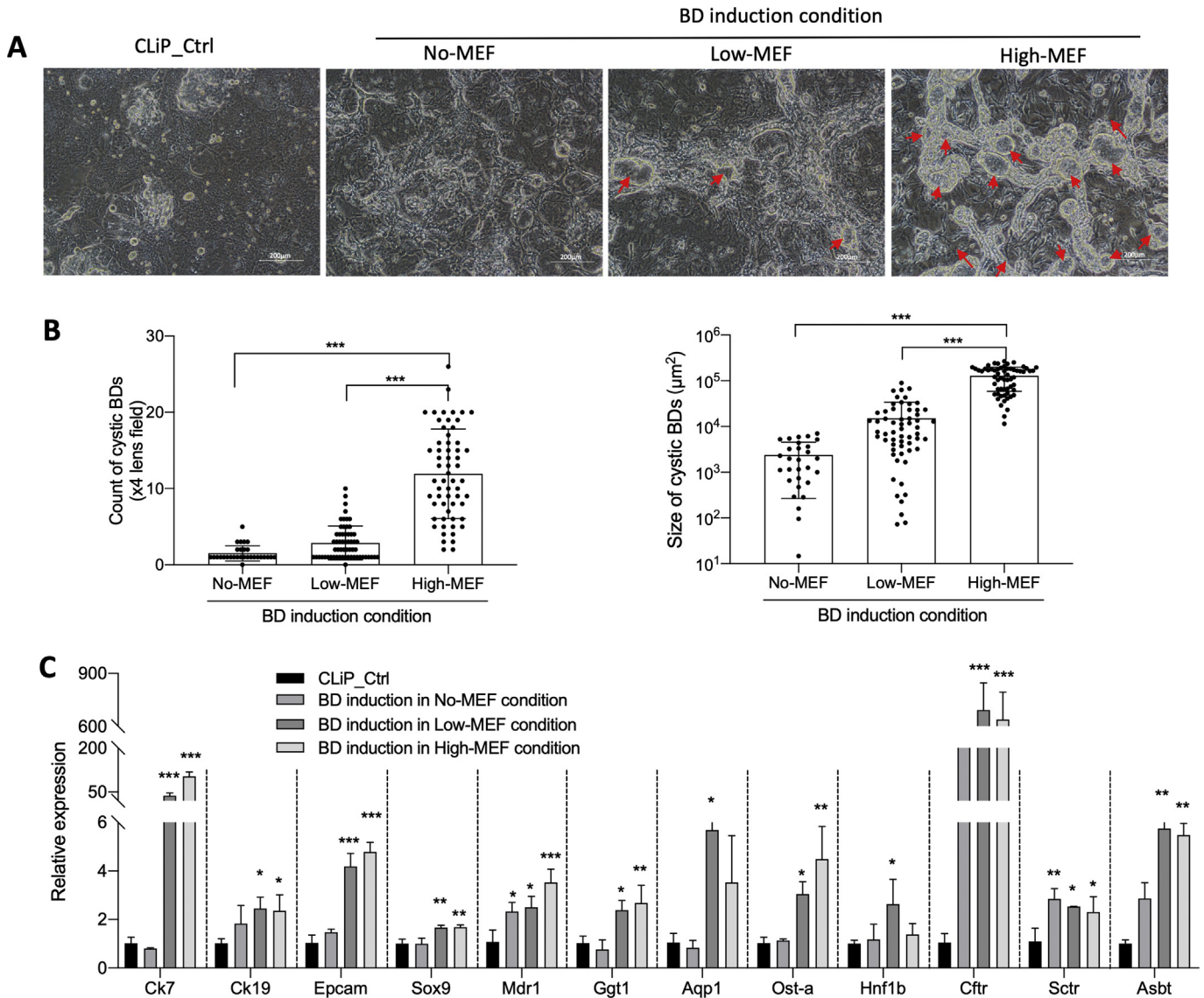
FIG. 4. MEF feeder cells affect bile duct (BD) formation. (A) Representative cell morphologies at day 12 among no-MEF, low-MEF, and high-MEF groups. Cells cultured in YAC-medium for the same period were used as the control (ctrl). The red arrows show the cystic BD structure. (B) The number and the size of cystic BDs in no-MEF, low-MEF, and high-MEF groups. Data were presented as the mean ± s.d. (lot = 3, n ≥ 10) and analyzed with a one-way ANOVA test, $^{***}p < 0.001$. (C) Relative biliary gene markers in no-MEF, low-MEF, and high-MEF groups were analyzed by RT-qPCR and compared to the samples cultured in YAC-medium for the same period as the control (ctrl). Data were presented as the mean ± s.d. (lot = 1, n = 3) and normalized to *Actb* as fold changes relative to the control, which was set as 1. Data were analyzed with a one-way ANOVA test, $^{*}p < 0.05$, $^{**}p < 0.01$, $^{***}p < 0.001$.

mRNA levels of *Notch1* and *Notch2* were upregulated in co-cultured with low-MEF, while this upregulation was not shown in high-MEF condition. Besides, the Notch target *Hes1* was correspondingly elevated in low-MEF condition, not in high-MEF condition. The Notch ligand *Jag1* was upregulated in both low-MEF and high-MEF conditions. This mRNA expression data showed that the MEF induced CLiP-derived BD structure through the Jag1-Notch1/2-Hes1 pathway (Fig. 7).

DISCUSSION

To date, studies of the potential applications of cholangiocytes have been limited because cholangiocytes make up a very small proportion of the liver cell population and have proven to be very difficult to isolate and maintain *in vitro* (19,20). At present, there are only a few models to accurately replicate them in culture (21). With the rise of stem cell research, studies have indicated that LPCs and/

or iPSCs can be used as an alternate and reproducible source that can be easily acquired and differentiated into cells with a biliary phenotype, such as cells under defined culture conditions as 3D structures (6,7,22,23). Because of their potential for long-term culture and repopulation capacity, CLiPs are another promising cell source that can be induced to adopt a cholangiocyte phenotype using a simple method (8,9).

In this study, we determined that the following key factors promoted the differentiation of CLiPs into BDs: (i) using earlier passages of primary-CLiPs, (ii) a 1-day preincubation period of CLiPs in YAC-medium before the induction step, (iii) 6 days of Matrigel addition at the second step, and (iv) using an appropriate MEF feeder cell number, i.e., using more MEF feeder cells to generate more cystic BD structures and less MEF feeder cells to obtain more tubular BD structures. The differentiated BDs expressed many mature biliary genes and proteins. Furthermore, we demonstrated that activating the Jag/Notch pathway affected
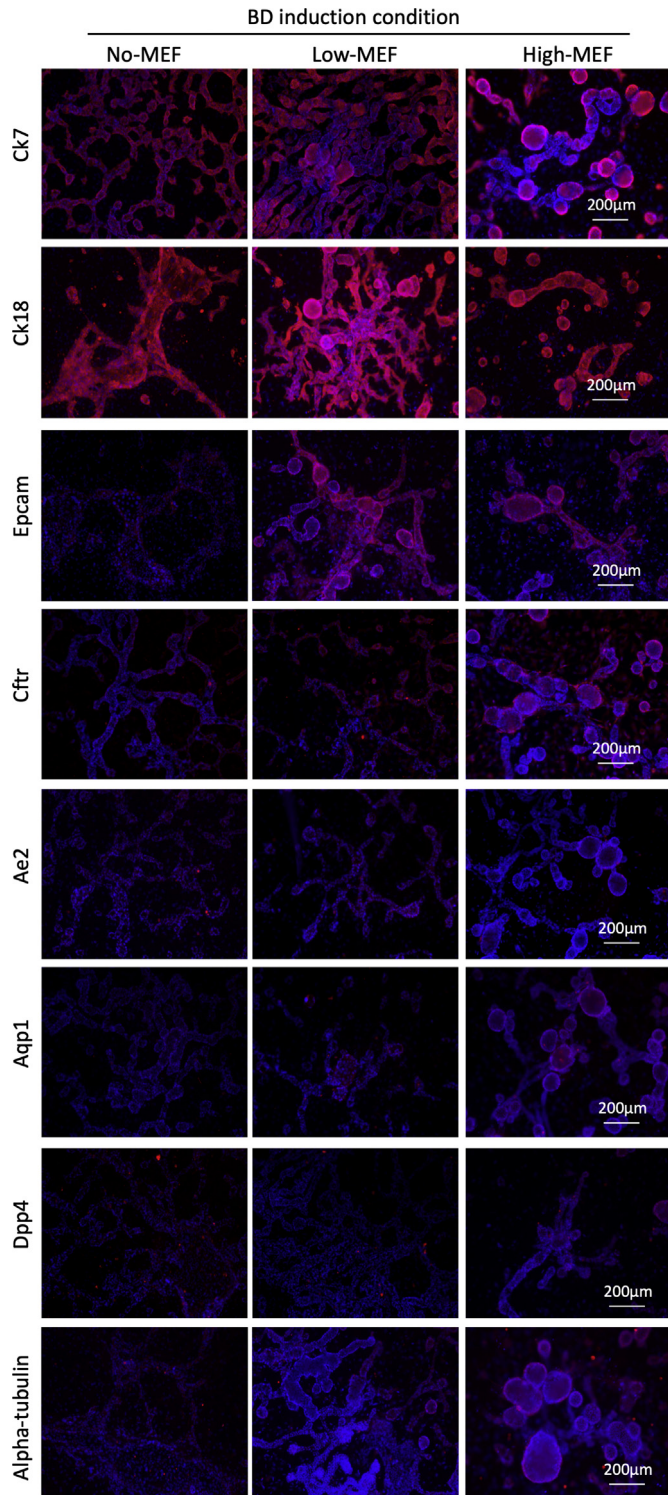
FIG. 5. MEF feeder cells affect bile duct protein expression. The biliary protein markers in no-MEF, low-MEF, and high-MEF groups were analyzed via immunostaining analysis.

BD formation. Therefore, this technique represents a platform for the future study of cholangiocytes *in vitro*.

According to the research conducted by Katsuda et al. (8), CLiPs can be stably cultured without obvious phenotypic alterations.

They defined the cells that were passaged >10 times as stable-CLiPs (8). Those long-termed cultured CLiPs can be stably expanded without diminishing their hepatic differentiation ability. In the present study, we also confirm that long-termed cultured CLiPs can be differentiated into cells with a biliary phenotype that express serval biliary markers. On the other hand, we found that using CLiPs of earlier passages resulted in the formation of better BD structures, including tubular and cystic BDs, and increased the expression of biliary marker genes compared with the stable CLiPs. This may partly be caused by the high proliferation rate in stable-CLiPs. Together, these results indicate the superiority of younger CLiPs for BD differentiation. Besides, CLiPs that have been passaged and converted from different individual hepatocytes may be different after subculture, which may affect the number of cells that attach to the dish. In those cases, extending the number of preincubation days in YAC-medium could be used to obtain enough cells before BD induction. However, it should be noted that a delay in BD formation was observed when the preincubation time was extended.

Protocols from the reported studies for biliary cell differentiation from stem cells always used a gel-embedded or 3D culture system (6,7,22,23). It has been considered that a 3D gel provides a space for tubulogenesis and the polarization of cholangiocytes. Similarly, the Matrigel in our system may provide the cells with a 3D space; however, the long-term addition of Matrigel may reduce typical tubular BD formation. Hence, the two-step protocol with the addition of Matrigel for 6 days at the second step is believed to benefit the formation of typical BDs in our system.

Ogawa et al. reported that the coculture of hepatoblasts with OP9 stromal cells, which are known to express different Notch ligands, including Jagged1, in a 3D culture system promoted cholangiocyte development (22). Here, we used MEFs as a 2D feeder layer for BD induction, and the data showed that MEF feeder cells affected BD formation and function, as well as gene and protein expression. In this study, MEF feeder cells offered the distribution of plated cells in a relative separated CLiP–CLiP interaction but a close interaction to MEF space. Compared to the group of BDs without MEF feeder (i.e., only CLiP–CLiP interaction), the BD in MEF feeder (i.e., CLiP–MEF interaction) showed more typical structures with both tubular and cystic BD structures, expressed much higher level of biliary gene makers (Fig. 4), and biliary proteins (Fig. 5), as well as Mdr1 transporter functionality (Fig. 6). Therefore, our data demonstrated that CLiP–MEF interaction is critical for biliary differentiation. It may imply that artificially plating or distributing the cells as treelike structures will produce the biliary tree structures. This means that we could control CLiP-derived duct formation by applying the 3D gel or 3D printing techniques in the future (24).

Even though the pathways that control biliary development are not fully understood, several essential signaling pathways and proteins that play important roles in BD morphogenesis have been confirmed (25–27). Another important morphogenetic cue comes from the Notch signaling pathway, which is well known for its regulation of biliary cell fate and morphogenesis of the developing biliary tree (14). In our differentiation system, data also showed the activation of Notch1/Notch2 and Jag1, confirming the important role of this pathway in BD formation by CLiPs.

Several protocols to induce iPSCs into cholangiocytes have been reported. Dianat et al. (7) determined the optimal conditions to drive the differentiation of human iPSCs derived from hepatoblasts into functional cholangiocyte-like cells using feeder-free and defined culture conditions, including the use of epidermal growth factor (EGF), IL-6, sodium taurocholate, and growth hormones. In a
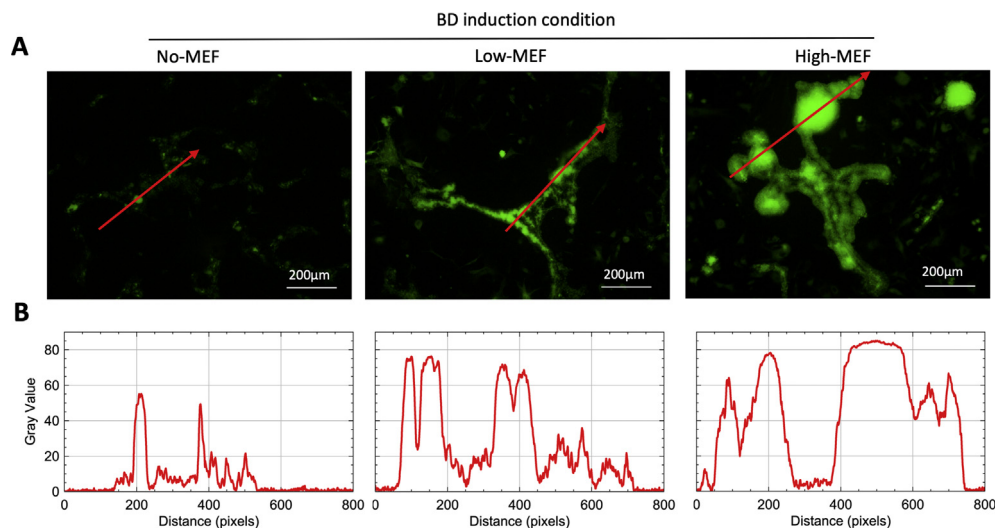
FIG. 6. MEF feeder cells affect bile duct function. (A) The rhodamine 123 assay was used in no-MEF, low-MEF, and high-MEF groups. (B) The fluorescence intensities along the red line in the images were measured and listed.
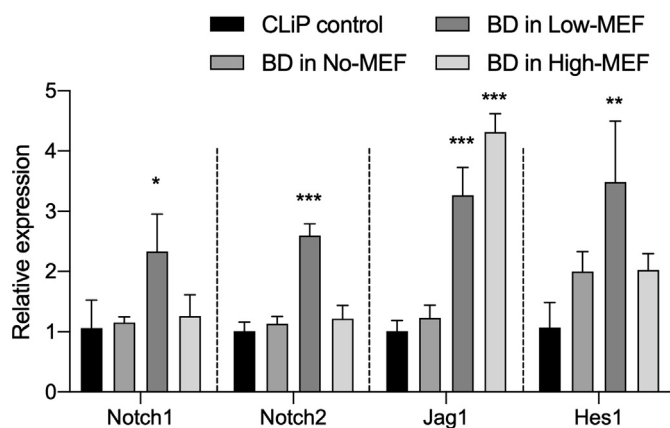

FIG. 7. MEF feeder cells affect the Jag/Notch pathway in CLiP-derived BD. The genes related to the Jag/Notch pathway in CLiP-derived BD induced on no-MEF, low-MEF, and high-MEF feeder conditions were analyzed via RT-qPCR and compared to the CLiP samples cultured in YAC-medium for the same period as control. Data were presented as the mean $\pm$ s.d. (lot = 1, n = 3) and normalized to *Actb* as fold changes relative to the control, which was set as 1. Data were analyzed with a one-way ANOVA test, $^*p < 0.05$, $^{**}p < 0.01$, $^{***}p < 0.001$.

3D matrix culture system, those cells developed epithelial/apico-basal polarity and formed biliary ducts and functional cysts. Afterward, Ogawa et al. (22) described a protocol that achieved the efficient differentiation of cholangiocytes from iPSCs by using a 3D coculture system of hepatoblasts with OP9 stromal cells and the combination of three different growth factors, including TGF-β, EGF, and HGF. Sampaziotis et al. (6) reported that exposure to FGF10, retinoic acid, and Activin A before 3D culture was important for cholangiocyte progenitor specification. Another study by De Assuncao et al. (23) fully characterized the cells *in vitro* and *in vivo* by exposing them to high concentrations of TGF-β and Jagged1. In our system of BD differentiation from CLiPs, we did not use growth factors or cytokines. Instead, we used Matrigel and MEF feeder cells, which is a much easier technique. Currently, we are trying to modify our protocol and apply it to human CLiP-derived BDs.

Two future applications of iPSC-derived cholangiocytes in basic and clinical research are the modeling of cholangiocyte diseases and the use of cholangiocytes in cell therapy, scaffolding, and bio-printing (21). Our CLiP-derived BD structures can be used to model the bile acid drainage system by immerging those cells into hepatocytes, which is an ongoing study in our laboratory.

In summary, we determined the optimal conditions for BD differentiation from rat CLiPs. Using our stable and efficient approach, BD structures can be used to study cholangiocyte diseases and regenerative medicine.

Supplementary data to this article can be found online at https://doi.org/10.1016/j.jbiosc.2020.07.009.

References

1. **Banales, J. M., Huebert, R. C., Karlsen, T., Strazzabosco, M., LaRusso, N. F., and Gores, G. J.:** Cholangiocyte pathobiology, Nat. Rev. Gastroenterol. Hepatol., **16**, 269–281 (2019).

2. **Pinto, C., Giordano, D. M., Maroni, L., and Marzioni, M.:** Role of inflammation and proinflammatory cytokines in cholangiocyte pathophysiology, Biochim. Biophys. Acta (BBA) – Mol. Basis Dis., **1864**, 1270–1278 (2018).

3. **Gordillo, M., Evans, T., and Gouon-Evans, V.:** Orchestrating liver development, Development, **142**, 2094–2108 (2015).

4. **Tian, L., Deshmukh, A., Ye, Z., and Jang, Y. Y.:** Efficient and controlled generation of 2D and 3D bile duct tissue from human pluripotent stem cell-derived spheroids, Stem Cell Rev. Rep., **12**, 500–508 (2016).

5. **Sampaziotis, F., De Brito, M. C., Geti, I., Bertero, A., Hannan, N. R. F., and Vallier, L.:** Directed differentiation of human induced pluripotent stem cells into functional cholangiocyte-like cells, Nat. Protoc., **12**, 814–827 (2017).

6. **Sampaziotis, F., De Brito, M. C., Madrigal, P., Bertero, A., Saeb-Parsy, K., Soares, F. A. C., Schrumpf, E., Melum, E., Karlsen, T. H., Bradley, J. A., and other 7 authors:** Cholangiocytes derived from human induced pluripotent stem cells for disease modeling and drug validation, Nat. Biotechnol., **33**, 845–852 (2015).

7. **Dianat, N., Dubois-Pot-Schneider, H., Steichen, C., Desterke, C., Leclerc, P., Raveux, A., Combettes, L., Weber, A., Corlu, A., and Dubart-Kupperschmitt, A.:** Generation of functional cholangiocyte-like cells from human pluripotent stem cells and HepaRG cells, Hepatology, **60**, 700–714 (2014).

8. **Katsuda, T., Kawamata, M., Hagiwara, K., Takahashi, R. U., Yamamoto, Y., Camargo, F. D., and Ochiya, T.:** Differentiation of terminally committed

hepatocytes to culturable bipotent progenitor cells with regenerative capacity, Cell Stem Cell, **20**, 41−55 (2017).

9. **Katsuda, T., Matsuzaki, J., Yamaguchi, T., Yamada, Y., Prieto-Vila, M., Hosaka, K., Takeuchi, A., Saito, Y., and Ochiya, T.:** Generation of human hepatic progenitor cells with regenerative and metabolic capacities from primary hepatocytes, Elife, **8**, e47313 (2019).

10. **Huang, Y., Sakai, Y., Hara, T., Katsuda, T., Ochiya, T., Adachi, T., Hidaka, M., Gu, W. L., and Eguchi, S.:** Development of bifunctional three-dimensional cysts from chemically induced liver progenitors, Stem Cells Int., **2019**, 3975689 (2019).

11. **Katsuda, T. and Ochiya, T.:** Chemically induced liver progenitors (CLiPs): a novel cell source for hepatocytes and biliary epithelial cells, Methods Mol. Biol., **1905**, 117−130 (2019).

12. **Seglen, P. O.:** Preparation of isolated rat liver cells, Methods Cell Biol., **13**, 29−83 (1976).

13. **Sakai, Y., Koike, M., Kawahara, D., Hasegawa, H., Murai, T., Yamanouchi, K., Soyama, A., Hidaka, M., Takatsuki, M., Fujita, F., Kuroki, T., and Eguchi, S.:** Controlled cell morphology and liver-specific function of engineered primary hepatocytes by fibroblast layer cell densities, J. Biosci. Bioeng., **126**, 249−257 (2018).

14. **Geisler, F. and Strazzabosco, M.:** Emerging roles of Notch signaling in liver disease, Hepatology, **61**, 382−392 (2015).

15. **McCright, B., Lozier, J., and Gridley, T.:** A mouse model of Alagille syndrome: Notch2 as a genetic modifier of Jag1 haploinsufficiency, Development, **129**, 1075−1082 (2002).

16. **Kodama, Y., Hijikata, M., Kageyama, R., Shimotohno, K., and Chiba, T.:** The role of notch signaling in the development of intrahepatic bile ducts, Gastroenterology, **127**, 1775−1786 (2004).

17. **Geisler, F., Nagl, F., Mazur, P. K., Lee, M., Zimber-Strobl, U., Strobl, L. J., Radtke, F., Schmid, R. M., and Siveke, J. T.:** Liver-specific inactivation of Notch2, but not Notch1, compromises intrahepatic bile duct development in mice, Hepatology, **48**, 607−616 (2008).

18. **Sparks, E. E., Huppert, K. A., Brown, M. A., Washington, M. K., and Huppert, S. S.:** Notch signaling regulates formation of the three-dimensional architecture of intrahepatic bile ducts in mice, Hepatology, **51**, 1391−1400 (2010).

19. **Joplin, R.:** Isolation and culture of biliary epithelial cells, Gut, **35**, 875−878 (1994).

20. **Joplin, R., Strain, A. J., and Neuberger, J. M.:** Immuno-isolation and culture of biliary epithelial cells from normal human liver, In Vitro Cell. Dev. Biol., **25**, 1189−1192 (1989).

21. **Cervantes-Alvarez, E., Wang, Y., Collin de l'Hortet, A., Guzman-Lepe, J., Zhu, J., and Takeishi, K.:** Current strategies to generate mature human induced pluripotent stem cells derived cholangiocytes and future applications, Organogenesis, **13**, 1−15 (2017).

22. **Ogawa, M., Ogawa, S., Bear, C. E., Ahmadi, S., Chin, S., Li, B., Grompe, M., Keller, G., Kamath, B. M., and Ghanekar, A.:** Directed differentiation of cholangiocytes from human pluripotent stem cells, Nat. Biotechnol., **33**, 853−861 (2015).

23. **De Assuncao, T. M., Sun, Y., Jalan-Sakrikar, N., Drinane, M. C., Huang, B. Q., Li, Y., Davila, J. I., Wang, R., O'Hara, S. P., Lomberk, G. A., and other 3 authors:** Development and characterization of human-induced pluripotent stem cell-derived cholangiocytes, Lab Invest., **95**, 684−696 (2015).

24. **Lewis, P. L., Yan, M., Su, J., and Shah, R. N.:** Directing the growth and alignment of biliary epithelium within extracellular matrix hydrogels, Acta Biomater., **85**, 84−93 (2019).

25. **Li, Z., White, P., Tuteja, G., Rubins, N., Sackett, S., and Kaestner, K. H.:** Foxa1 and Foxa2 regulate bile duct development in mice, J. Clin. Invest., **119**, 1537−1545 (2009).

26. **Clotman, F., Lannoy, V. J., Reber, M., Cereghini, S., Cassiman, D., Jacquemin, P., Roskams, T., Rousseau, G. G., and Lemaigre, F. P.:** The onecut transcription factor HNF6 is required for normal development of the biliary tract, Development, **129**, 1819−1828 (2002).

27. **Tan, X., Yuan, Y., Zeng, G., Apte, U., Thompson, M. D., Cieply, B., Stolz, D. B., Michalopoulos, G. K., Kaestner, K. H., and Monga, S. P. S.:** B-catenin deletion in hepatoblasts disrupts hepatic morphogenesis and survival during mouse development, Hepatology, **47**, 1667−1679 (2008).